Stabilizing Interactions and Coordination in Cationic Zirconocene Complexes: Cp_2ZrL^+. A MO Theoretical Study

Rolf Gleiter,*,† Isabella Hyla-Kryspin,† Shuqiang Niu,† and Gerhard Erker‡

Organisch-Chemisches Institut der Universität Heidelberg, Im Neuenheimer Feld 270, D-69120 Heidelberg, Germany, and Organisch-Chemisches Institut der Universität Münster, Corrensstrasse 40, D-48149 Münster, Germany

Received December 1, 1992

The results of ab initio RHF and RMP2 geometry optimization on the model compounds of the postulated intermediates in Ziegler–Natta catalysis $Cl_2ZrCH_2CH_3^+$ (**3**) and $Cl_2ZrCH{=}CH_2^+$ (**4**) and for comparison on three neutral complexes $Cl_2Zr(X)CH{=}CH_2$, X = H (**5**), CH_3 (**6**), Cl (**7**), show that these species are stabilized through a three-center 2-electron Zr–H_β–C interaction. In **5**–**7** this interaction is regiospecific and takes place either cis (**5a**) or trans (**6b**, **7b**) to the Zr–X bond, depending on the steric repulsion between X and H_β. The examination of the potential energy surface on the basis of extended Hückel calculations on substituted species $Cp_2ZrC(R_1){=}CH(R_2)^+$, R_1 = $SiMe_3$ (**8**), CMe_3 (**9**) and R_2 = H (**a**), Me (**b**), SiH_3 (**c**), CMe_3 (**d**), $SiMe_3$ (**e**), Ph (**f**), reveals that **8** and **9** can be stabilized through either γ-Si (C)–C or β-CH agostic interactions, depending on the subtle balance between the electronic and steric effects on R_1 and R_2.

I. Introduction

Organometallic compounds with a coordinatively unsaturated metal center are known to be stabilized by the M—H—C three-center 2-electron interaction.[1] In many cases this agostic interaction leads to CH bond activation and is therefore a very important topic of organometallic chemistry. Intramolecular coordination of a CH bond requires a suitable metal acceptor orbital and is of electronic origin. The inclination to satisfy the 18-electron rule has been considered to be a necessary driving force for the agostic interaction. In complexes with a strongly electrophilic metal center such as $(dmpe)Cl_3TiCH_3$ and $(dmpe)Cl_3TiC_2H_5$[2] the electronic origin seems to dominate the M—H—C agostic interaction.[3] Recently, we have shown that in the case of the much less electrophilic 16-electron $Cp_2Zr(Cl)$–alkenyl complexes, the stabilizing M—H—C agostic interaction depends on electronic *and* steric effects.[4] In the present study we have examined the factors which contribute to the stabilization of the more electrophilic 14-electron cationic zirconocene complexes Cp_2ZrL^+ (L = ethyl, vinyl). The cationic species Cp_2ML^+ (M = group 4 metals) are postulated to be catalysts in the polymerization reactions of alkenes.[5] The first isolated intermediates of a Ziegler catalyst system, compounds **1** and **2**, have been reported and characterized by X-ray crystallography recently.[6] Ab initio MO calculations on a model compound for **1**, $Cl_2Ti(CH_3H_2Si)C{=}CH_2^+$, suggest that **1** is stabilized through a γ-C—Si and two γ-C—H agostic interactions.[7a] Similar interactions were postulated for **2** with the exception that only one CH σ-bond contributes to the stabilization.[6b]

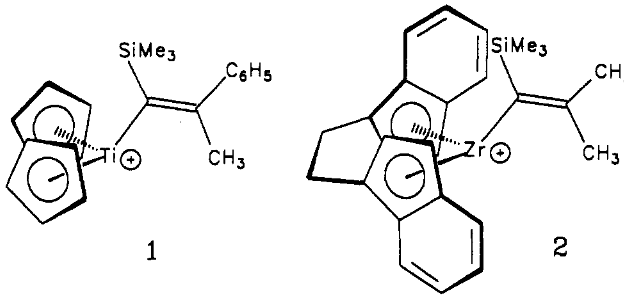

1 2

(1)

In our investigations we have focused on three questions: (a) which agostic interactions stabilize the Cp_2ZrL^+ species, (b) what is the origin of the stabilizing interactions, and (c) what is the coordination fashion of L to the metal

---

† Organisch-Chemisches Institut der Universität Heidelberg.

‡ Organisch-Chemisches Institut der Universität Münster.

(1) For a recent comprehensive review see: Brookhart, M.; Green, M. L. H.; Wong, L.-L. *Prog. Inorg. Chem.* **1988**, *36*, 1. Crabtree, R. H.; Hamilton, D. G. *Adv. Organomet. Chem.* **1988**, *28*, 299.

(2) (a) Dawoodi, Z.; Green, M. L. H.; Mtetwa, V. S. B.; Prout, K. *J. Chem. Soc., Chem. Commun.* **1982**, *802*, 1410. (b) Dawoodi, Z.; Green, M. L. H.; Mtetwa, V. S. B.; Prout, K.; Schultz, A. J.; Williams, J. M.; Koetzle, T. F. *J. Chem. Soc., Dalton Trans.* **1986**, *1629*.

(3) (a) Koga, N.; Obara, S.; Morokuma, K. *J. Am. Chem. Soc.* **1984**, *106*, 4625. (b) Eisenstein, O.; Jean, Y. *J. Am. Chem. Soc.* **1985**, *107*, 1177. (c) Demolliens, A.; Jean, Y.; Eisenstein, O. *Organometallics* **1986**, *5*, 1457.

(4) (a) Hyla-Kryspin, I.; Gleiter, R.; Krüger, C.; Zwettler, R.; Erker, G. *Organometallics* **1990**, *9*, 517. (b) Erker, G.; Zwettler, R.; Krüger, C.; Hyla-Kryspin, I.; Gleiter, R. *Organometallics* **1990**, *9*, 524.

(5) (a) Dyachkovskii, F. S.; Shilova, A. K.; Shilov, A. E. *J. Polym. Sci., Part C* **1967**, *16*, 2333. (b) Eisch, J. J.; Galle, J. E.; Piotrowski, A. M. In *Transition Metal Catalyzed Polymerization*; *Alkenes and Dienes*; Quirk, R. P.; Ed.; Harwood: New York, 1983; Part B, p 779. (c) Gassman, P. G.; Callstrom, M. R. *J. Am. Chem. Soc.* **1987**, *109*, 7875. (d) Eisch, J. J.; Boleslawski, M. P.; Piotrowski, A. M. In *Transition Metals and Organometallics as Catalysts for Olefin Polymerization*; Kaminsky, W., Linn, M., Eds.; Springer-Verlag: Berlin, Heidelberg, 1988; p 371. (e) Eisch, J. J.; Caldwell, K. R.; Werner, S.; Krüger, C. *Organometallics* **1991**, *10*, 3417. (f) Jordan, R. F. *Adv. Organomet. Chem.* **1991**, *32*, 325.

(6) (a) Eisch, J. J.; Piotrowski, A. M.; Brownstein, S. K.; Gabe, E. J.; Florence, L. L. *J. Am. Chem. Soc.* **1985**, *107*, 7219. (b) Horton, A. D.; Orpen, A. G. *Organometallics* **1991**, *10*, 3910. (c) For a related example see: Jordan, R. F.; LaPointe, R. E.; Bradley, P. K.; Baenziger, N. C. *Organometallics* **1989**, *8*, 2892.

(7) (a) Koga, N.; Morokuma, K. *J. Am. Chem. Soc.* **1988**, *110*, 108. See for a comparison: (b) Jordan, R. F.; Taylor, D. F.; Baenziger, N. C. *Organometallics* **1990**, *9*, 1546. (c) Jordan, R. F.; Bradley, P. K.; Baenziger, N. C.; LaPointe, R. E. *J. Am. Chem. Soc.* **1990**, *112*, 1289. (d) Jolly, C. A.; Marynick, D. S. *J. Am. Chem. Soc.* **1989**, *111*, 7968. Brintzinger, H. H. In *Organic Synthesis via Organometallics* Dötz, K. H., Hoffmann, R. W. Eds.; Vieweg: Braunschweig, 1990; p 33 and references therein.

0276-7333/93/2312-3828$04.00/0

Chart I

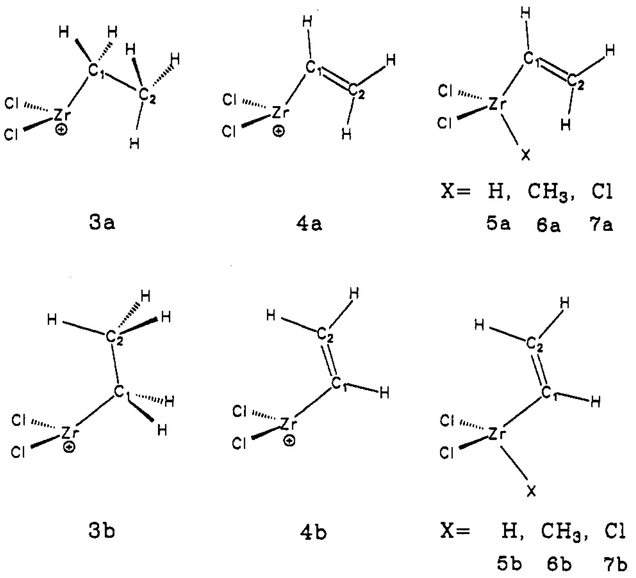

center? To answer the above questions we have carried out geometry optimization for the model compounds **3**–**7**.

The structures **3b**–**7b** can be derived from **3a**–**7a** by rotating L (ethyl or vinyl) around the Zr–C bond. For **3a**–**7a** one can expect β-CH agostic interactions and for **3b**–**7b** the corresponding α-CH interactions. To examine the influence of the substituents in the vinylic part, we have carried out extended Hückel calculations for the model compounds **8a**–**8f** and **9a**–**9f**. One can suppose that

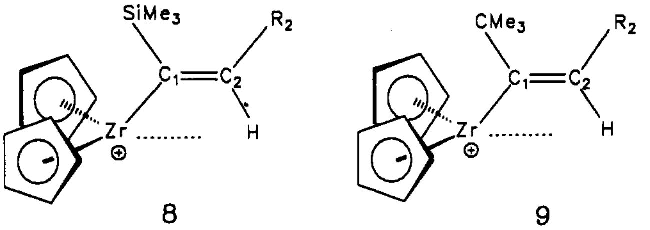

8 9

R_2=H, Me, SiH$_3$, CMe$_3$, SiMe$_3$, Ph
a b c d e f

(2)

the substitution of the "nonagostic" hydrogens in **4a** will change the character of the stabilizing interactions and perhaps the coordination fashion of the ligand to the metal fragment also. The latter may play an important role in the stereoselectivity of alkene polymerization by metallocene catalysts.

II. Computational Details

The geometry optimizations were carried out using the energy gradient technique at the ab initio restricted Hartree–Fock (RHF) and restricted second-order Moller–Plesset (RMP2) level.[8] We used two basis sets, denoted later as BS1 and BS2. The BS1 is a minimal STO-3G basis for all atoms. The BS2 is designed as follows: for zirconium we selected a (14, 9, 7) basis set obtained by adding a p-type orbital exponent 0.12 to the standard set optimized by Hyla-Kryspin et al.[9] The contraction is [6, 4, 4], corresponding to a single-ξ description for the inner shells and the 5p shell, double-ξ for 5s, and triple-ξ for 4d. The most diffuse exponent for the valence d shell is 0.134 708, and the maximum of the associated density distribution is located 1.76 Å from the nucleus. Basis sets of respective size (10, 6), (9, 5), and (4) were used for chlorine, carbon, and hydrogen and contracted to split valence.[10] In order to estimate the correlation effects and for better energetics, with both basis sets we have carried out RMP2 perturbation calculations with geometries optimized at the RHF level (RMP2//RHF/BS1, RMP2//RHF/BS2) and with BS1 we performed geometry optimization at the RMP2 level (RMP2/BS1). In the ab initio calculations the Cp ligand was replaced by chlorine; this simplification has been found to be a reasonable structural model.[7a,11]

The extended Hückel calculations were carried out with standard parameters for all atoms.[12]

III. Results and Discussion

A. Ab Initio Calculations on Model Compounds 3–7. The fully optimized geometries (RHF/BS2) of two cationic complexes $Cl_2Zr(ethyl)^+$ (**3a**) and $Cl_2Zr(vinyl)^+$ (**4a**) and, for means of comparison, of three neutral molecules $Cl_2Zr(X)(vinyl)$ with X = H (**5a**), CH_3 (**6a**), and Cl (**7a**) are shown in Figure 1. It is noted that the calculated Zr–C–C bond angle of **3a** (87.8°) is much smaller than that expected for sp^3-hybridization (109.47°); it deviates only slightly from the experimental value of 85.8° found in $(dmpe)Cl_3TiC_2H_5$.[2a] The same is found for **4a** and **5a** but not for **6a** and **7a**. The optimized Zr–C–C bond angles of **4a** (91.5°) and **5a** (96.0°) are much smaller than the expected value for an sp^2 center (120°), and it scarcely deviates from the experimental values (88–90°) found for the neutral β-CH agostic zirconocene complexes.[4] The distance between the Zr atom and the H_β of the ethyl group in **3a** (2.176 Å) or of the vinyl group in **4a** (2.297 Å) and **5a** (2.492 Å) deviates strongly from the values found for the neutral species **6a** (3.287 Å) and **7a** (3.250 Å). The small distances for **3a**, **4a**, and **5a** are indicative for a direct Zr–H_β interaction. The CH_β bond in **3a** (1.140 Å) is by 0.06 Å longer than the other CH bonds in the same ethyl group. The same was found in the model calculations of Koga et al. for the Ti complex.[3a] The length of the CH_β bond in **4a** (1.109 Å) is about 0.04 Å longer as compared to those in **6a** and **7a** or to the other CH bonds in the same vinyl group.

The same is valid for **5a**, but to a lower extent. The structural features of **3a**–**7a** suggest the existence of the β-CH agostic interactions in **3a**–**5a** but not in **6a** and **7a**. In the neutral complexes **6a** and **7a** the repulsion between X (CH_3 or Cl) and H_β does not allow for a β-CH agostic interaction. It can be overcompensated for by the use of bulky substituents in the vinylic part only. As a good example serve the structural features of the β-CH agostic

---

[8] We used the GAUSSIAN 86 program by M. J. Frisch, J. S. Binkley, H. B. Schlegel, K. Raghavachari, C. F. Melius, R. L. Martin, J. J. P. Stewart, F. W. Bobrowicz, C. M. Rohlfing, L. R. Kahn, D. J. Defrees, R. Seeger, R. A. Whiteside, D. J. Fox, E. M. Fleuder, J. A. Pople, Carnegie-Mellon Quantum Chemistry Publishing Unit, Pittsburgh, PA, 1984.

(9) Hyla-Kryspin, I.; Demuynck, J.; Strich, A.; Bénard, M. *J. Chem. Phys.* **1981**, *75*, 3954.

(10) (a) Roos, B.; Siegbahn, P. *Theor. Chim. Acta* **1970**, *17*, 209. (b) Dunning, T. H., Jr. *J. Chem. Phys.* **1970**, *53*, 2823. (c) Huzinaga, S. *J. Chem. Phys.* **1965**, *42*, 1293.

(11) (a) Rappé, A. K.; Goddard, W. A., III. *J. Am. Chem. Soc.* **1982**, *104*, 297. (b) Upton, T. H.; Rappe, A. K. *J. Am. Chem. Soc.* **1985**, *107*, 1206.

(12) (a) Summerville, R. H.; Hoffmann, R. *J. Am. Chem. Soc.* **1976**, *98*, 7240. (b) Hofmann, P.; Stauffert, P.; Schore, N. E. *Chem. Ber.* **1982**, *115*, 2153.

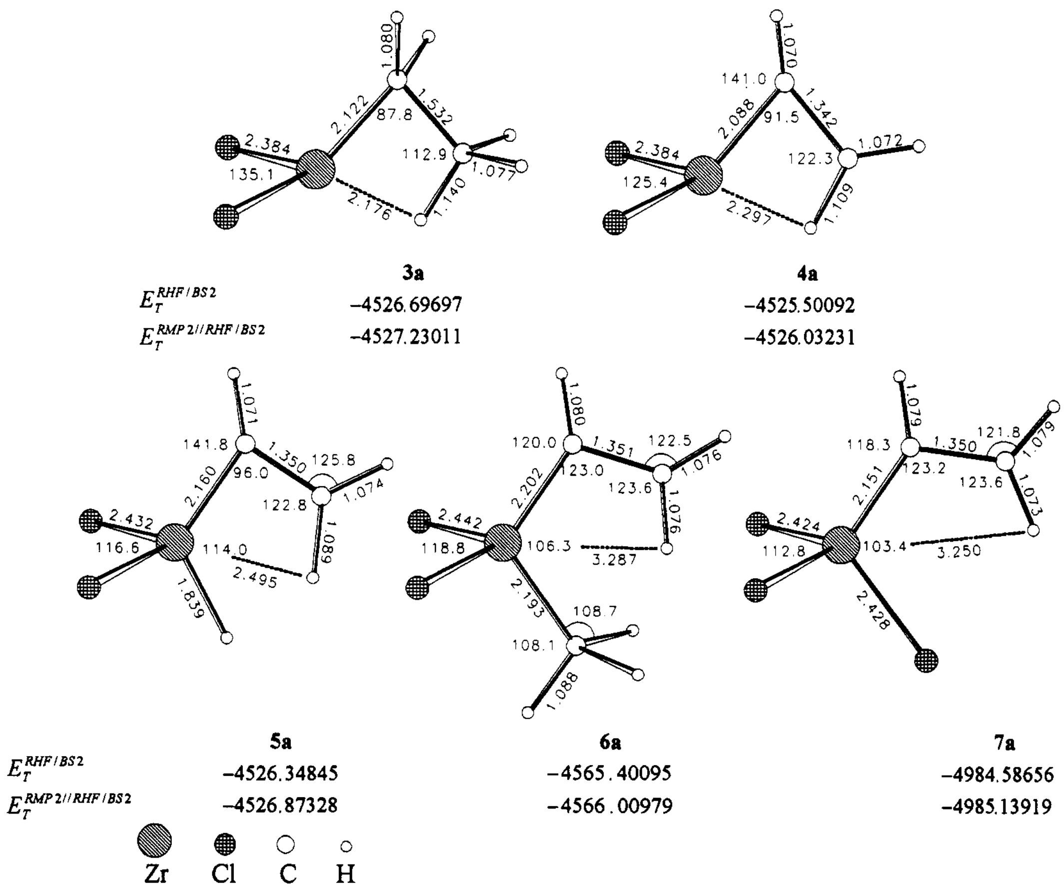

Figure 1. Optimized (RHF/BS2) structural parameters of **3a**–**7a**. The values are given in angstroms and degrees, respectively.

Table I. Total Energies (au) and Optimized Structural Parameters (RHF/BS1) of 3a–7a[a]

	3a	4a	5a	6a	7a
Zr–C_α	2.178	2.117	2.159	2.211	2.201
Zr–C_β	2.581	2.441	2.546	3.079	3.101
Zr–H_β	2.139	2.145	2.260	3.159	3.209
C_α–C_β	1.542	1.324	1.318	1.321	1.323
C_α–H_α	1.087	1.088	1.084	1.087	1.088
C_β–H_β	1.163	1.142	1.111	1.085	1.085
$\angle ZrC_\alpha C_\beta$	86.2	87.2	90.9	123.8	121.6
$E_T^{RHF/BS1}$	−4490.147 20	−4488.934 18	−4489.715 54	−4528.313 92	−4943.852 18
$E_T^{RMP2//RHF/BS1}$	−4490.370 20	−4489.172 49	−4489.944 02	−4528.590 44	−4944.084 51

[a] Distances are given in angstroms; angles, in degrees.

complex $Cp_2Zr(Cl)SiMe_3C{=}CHPh$.[4] Thus steric and electronic influence is necessary to reduce the $ZrC_\alpha C_\beta$ bond angle and to bring the CH_β bond and the metal center close together. In **5a** the hydrogen ligand at Zr is not so space-demanding as chlorine or CH_3; therefore **5a** shows a structural deformation similar to that of **4a**. For a comparison, we present in Table I some of the RHF/BS1 optimized structural parameters of **3a**–**7a**. It is well-known that minimal basis functions give a large basis set superposition error (BSSE) which first of all results in overestimation of dissociation energy (not discussed in this paper). Erroneous results can occur also in these cases, where particular atoms of a molecule are described by not well balanced Gaussian functions, e.g. by using minimal BS for some atoms and split BS for the other ones. In BS1 and BS2 each atom is described by properly balanced Gaussian functions and as we are interested in structural differences among **3**–**7**, it is not surprising for us that both basis sets predict similar structural behaviors of the model compounds and the results fall into the range of acceptable bond lengths and bond angles. However, as **3**–**7** are *model compounds*, we do not intend to compare them with those of really existing molecules. In order to explore the electronic nature of the possible β-CH agostic interaction in **3a**–**5a**, we have calculated the energy difference ΔE, the difference of the overlap populations ΔOP, and the difference of the electron density at the Zr atom Δq, between the fully optimized and standard structures (see Table II). The standard structures were optimized under the constraint that the $ZrC_\alpha C_\beta$ bond angle was fixed at 109.5° (**3a**) or 120° (**4a**, **5a**) and with all other parameters relaxed. The calculated structural parameters (RHF/BS2)

Table II. Characteristics of the β-CH Agostic Interaction in 3a–5a[a]

	3a		4a		5a	
	BS1	BS2	BS1	BS2	BS1	BS2
ΔE^{RHF} (kcal/mol)	−11.0	−10.2	−13.0	−7.1	−1.4	−1.3
$\Delta E^{RMP2//RHF}$ (kcal/mol)	−13.8	−13.1	−16.9	−12.0	−5.6	−5.2
ΔOP_{Zr-C_β}	0.03	0.03	0.05	0.05	0.02	0.03
ΔOP_{Zr-H_β}	0.08	0.08	0.08	0.05	0.03	0.02
$\Delta OP_{C_\beta-H_\beta}$	−0.08	−0.10	−0.08	−0.09	−0.03	−0.04
$\lvert\Delta q^{Zr}\rvert$	0.07	0.14	0.04	0.17	0.04	0.10

[a] Δ ≡ difference between the agostic and standard structure.

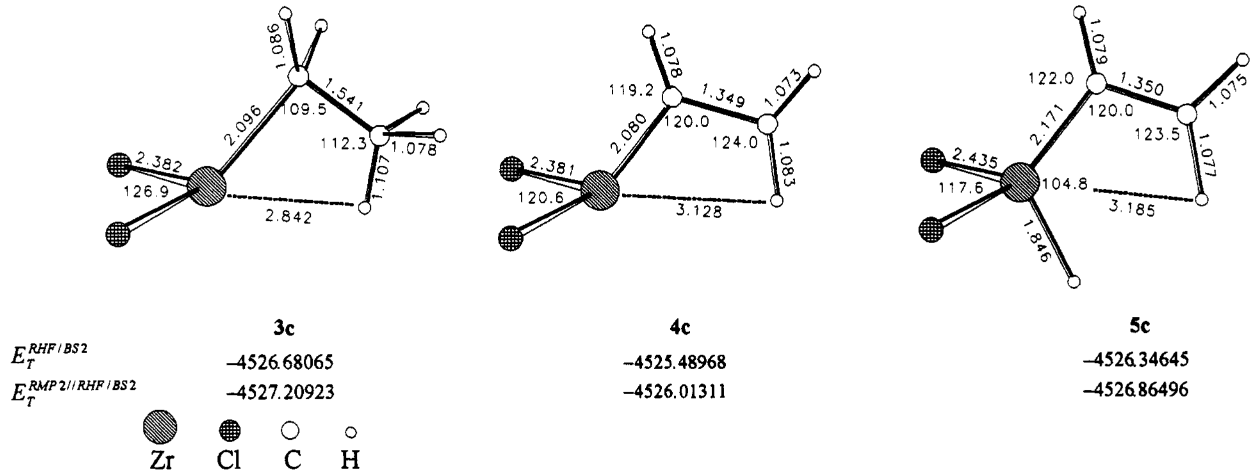

	3c	4c	5c
$E_T^{RHF/BS2}$	−4526.68065	−4525.48968	−4526.34645
$E_T^{RMP2//RHF/BS2}$	−4527.20923	−4526.01311	−4526.86496

Figure 2. Optimized RHF/BS2 structural parameters of the standard structures **3c**–**5c**. The values are given in angstroms and degrees, respectively.

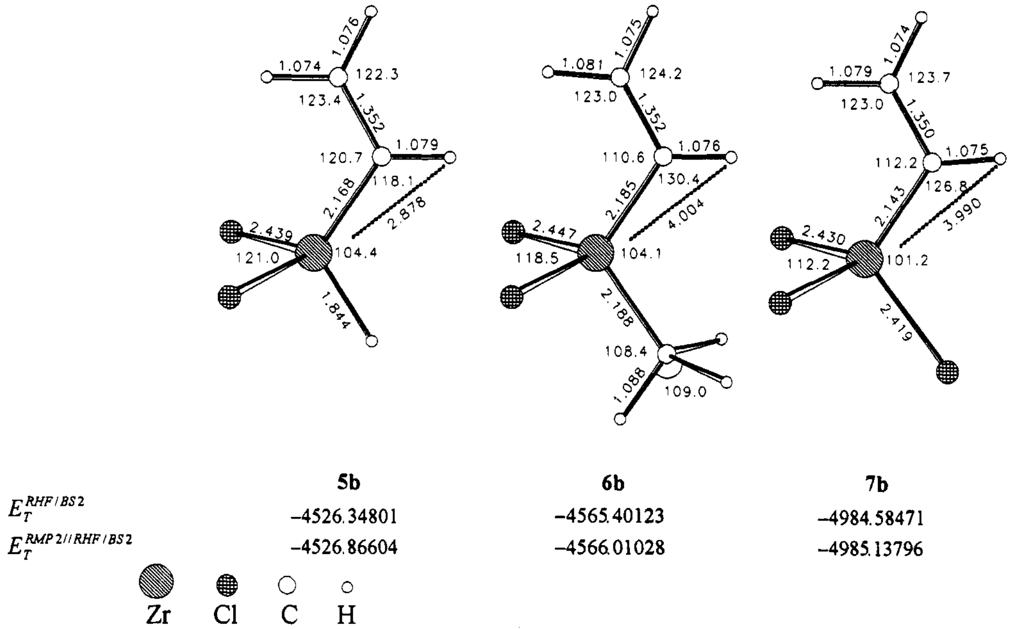

	5b	6b	7b
$E_T^{RHF/BS2}$	−4526.34801	−4565.40123	−4984.58471
$E_T^{RMP2//RHF/BS2}$	−4526.86604	−4566.01028	−4985.13796

Figure 3. Optimized (RHF/BS2) structural parameters of **5b**–**7b**. The values are given in angstroms and degrees, respectively.

of the standard structures **3c**–**5c** are shown in Figure 2. The CH_β bond in **3c**–**5c** is 0.03–0.01 Å shorter than that in **3a**–**5a**. The distorted structures are 10.2 (**3a**), 7.1 (**4a**), and 1.3 (**5a**) kcal/mol more stable as compared to the standard ones (RHF/BS2). The RMP2//RHF/BS2 calculations predict a stabilization of 13.1 (**3a**), 12.0 (**4a**), and 5.2 (**5a**) kcal/mol.

The distortion leads to an increase of the electron density at the Zr atom, an increase of the overlap population for the Zr–C_β and Zr–H_β bonds, and a decrease of the overlap population in the CH_β σ-bond. All the above features are in accord with the donor–acceptor properties of the β-CH agostic interaction and confirm its electronic origin. For **3a**–**5a** bulky substituents are not necessary to enforce the β-CH agostic interaction as in **6a** and **7a**. However, bulky substituents may change the character of the stabilizing interactions. This will be discussed in the next part. The fully optimized structures (RHF/BS2) of **5b**–**7b** are shown in Figure 3. During the geometry optimization, **3b** and **4b** converge obviously to the β-CH agostic structures **3a** and **4a**. The distance between the Zr atom and H_α in **5b**–**7b** is quite long (2.878 Å in **5b**, 4.004 Å in **6b**, 3.990 Å in **7b**), and the distance C–H_α is of the same order as the other CH bond. Both of the above features exclude a direct Zr–H_α interaction, i.e. the α-CH agostic interaction. A comparison of the RMP2//RHF/BS2 total energies suggests that structure **5a** is 4.5 kcal/mol more stable than **5b**. The difference of the total energies for **6a**, **7a** and **6b**, **7b** is too small to predict a preferred geometry. However, the structures **6b** and **7b** are characterized by a reduced $ZrC_\alpha C_\beta$ bond angle (110.6° in **6b**, 112.2° in **7b**), suggesting the possibility of a weak β-CH agostic interaction, trans to the Zr–X (X = CH_3, Cl) bond.

Recently, Weiss et al. showed that electron correlation is essential for a theoretical verification of agostic interactions.[13] In order to verify which agostic interactions stabilize the model compounds **5**–**7** we have carried out RMP2/BS1 geometry optimization, and the results are summarized in Table III. The calculated RMP2/BS1 structural parameters exclude any Zr–H_α agostic interaction. However, for **6b** and **7b** the distances Zr–H_β and Zr–C_β are significantly shorter and C_β–H_β is longer than in **6a** and **7a** (Table III). Again, the structure **5a** is 4.8 kcal/mol more stable than **5b**, but **6b** and **7b** are now more stable by 1.2 and 2.4 kcal/mol, respectively. The RMP2/

---

(13) Weiss, H.; Haase, F.; Ahlrichs, R. *Chem. Phys. Lett.* **1992**, *194*, 492.

Table III. Total Energies (au) and Optimized Structural Parameters (RMP2/BS1) of 5a–7a and 5b–7b[a]

	5a	5b	6a	6b	7a	7b
Zr–C_α	2.163	2.165	2.202	2.168	2.204	2.158
Zr–H_α	3.166	3.152	3.035	3.147	2.963	3.151
Zr–C_β	2.496	2.612	3.013	2.641	3.127	2.577
Zr–H_β	2.156	2.368	3.024	2.413	3.266	2.311
C_α–C_β	1.356	1.366	1.367	1.367	1.367	1.365
C_α–H_α	1.102	1.103	1.106	1.103	1.108	1.103
C_β–H_β	1.143	1.123	1.104	1.120	1.103	1.127
$\angle ZrC_\alpha H_\alpha$	150.1	147.6	130.1	146.5	123.5	148.3
$\angle ZrC_\alpha C_\beta$	87.2	92.6	113.1	94.0	120.4	91.2
$E_T^{RMP2/BS1}$	–4489.948 71	–4489.941 12	–4528.596 13	–4528.598 06	–4944.089 16	–4944.093 04

[a] Distances are given in angstroms; angles, in degrees.

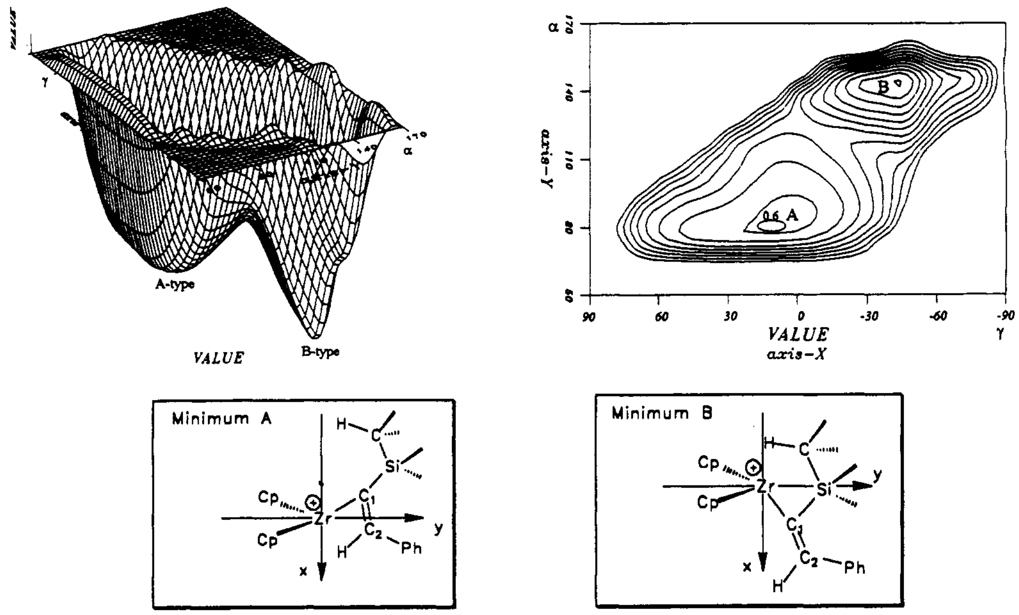

Figure 4. Energy contour map of **8f** as a function of α and γ. The contour lines are equidistant at 0.2 eV. The values are derived from an extended Hückel calculation.

BS1 results confirm the existence of the β-CH agostic interaction cis to the Zr–H bond in **5a** and suggest a β-CH agostic interaction trans to the Zr–X (X = CH_3, Cl) bond in **6b** and **7b**.

To conclude this section, we point out that the results of RHF or RMP2//RHF calculations concerning the energetics and structural behavior are similar for both basis sets, probably as a result of a good balance among the Gaussian functions describing particular atoms in BS1 and BS2. Although the RHF approximation is qualitatively correct to describe an agostic interaction, in some cases the consideration of electron correlation can be necessary.

B. Extended Hückel Calculations on Substituted Cationic Zirconocene Complexes. It is obvious that a complete geometry optimization for **8** and **9** is a prohibitive task. But, as we are primarily interested in the coordination fashion of the $R_1C{=}CR_2H$ ligand, we varied only the angles α and γ (see formula 3). All other parameters

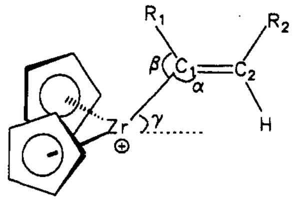

(3)

have been kept fixed at experimental values of similar neutral complexes.[4] We assume that the angles SiC_1C_2 in **8** and CC_1C_2 in **9** are equal to 120°. For each model compound the geometry search interestingly leads to two distinct minima on the (α, γ) energy surface. As an example we have shown in Figure 4 the energy contour map in the case of **8f**. The geometry of minimum A (α ≪ 120°) shows typical features of the β-CH agostic structure. The geometry of minimum B (α ≫ 120°) is close to the X-ray structure of **1** and **2**. For all model compounds **8** the B-type structures are 6.7–15.9 kcal/mol more stable with respect to A. For the complexes **9**, with exception of **9a** and **9d**, the β-CH agostic structure of minimum A is more stable (Table IV).

Table IV. Energy Difference ΔE(A–B) (kcal/mol) between the Geometries A and B of 8 and 9

	R_2					
R_1	H	CMe_3	Ph	Me	$SiMe_3$	SiH_3
$SiMe_3$	15.9	13.0	11.8	10.7	8.7	6.7
CMe_3	10.6	0.0	–1.1	–3.0	–3.0	–4.9

To find the reason for this difference, we need to compare the possible stabilizing interactions prevailing in both structures. Both conformations have the same highly electrophilic Zr center, and one can suppose that the coordination is influenced by different donor strengths of the particular σ-bonds. We have adopted Hoffmann's fragment MO approach[14] allowing interactions between the Cp_2Zr^{2+} unit (**10**) and the $Me_3Si{-}C{=}CH_2^-$ ligand (**11**) in the standard (α = 120°) and optimized geometries (α

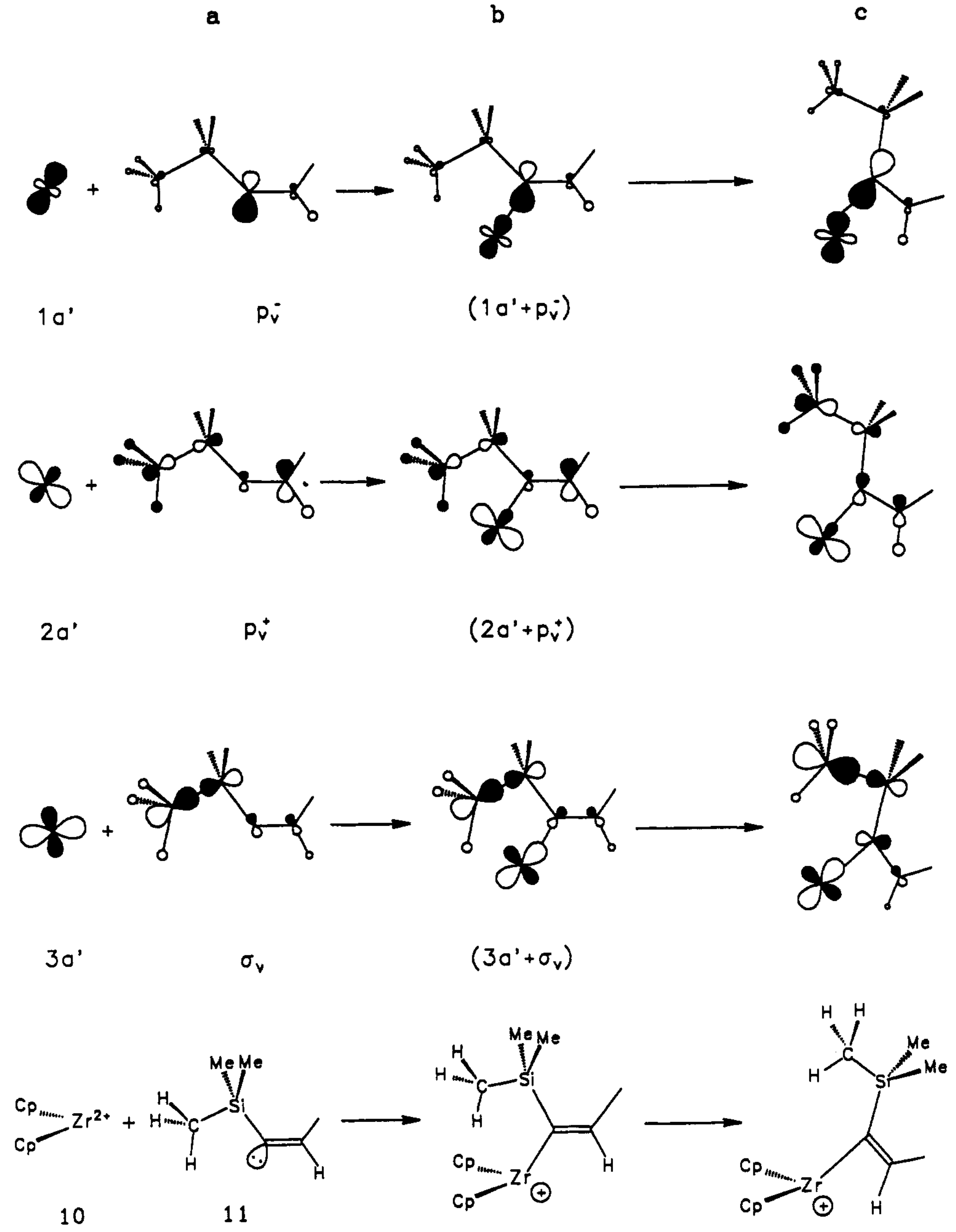

Figure 5. (a) Schematic drawing of the lowest unoccupied MOs of a Cp_2Zr^{2+} unit (**10**) and the highest occupied σ MOs of a $(CH_3)_3Si—C{=}CH_2^-$ unit (**11**). (b) Highest occupied MOs of **8a** (conformation A) assuming no agostic interactions. (c) Highest occupied σ MOs of **8a** assuming minimum A and agostic interactions.

$\neq 120°$). The familiar valence MOs of a bent Cp_2M (C_{2v}) fragment are described in detail in the literature.[14] For **11** the calculations predict four high lying occupied MOs: p_v^-, π_v^{cc}, p_v^+, and σ_v. Three of them (p_v^-, p_v^+, σ_v) are shown at the left of Figures 5 and 6. The HOMO (p_v^-) describes the lone pair orbital at carbon C_1. The MOs p_v^+ and σ_v describe the CH and SiC σ-bonds. Fragment **10** has five unoccupied MOs which are strongly localized at the metal center. The most important are the low lying LUMO ($1a_1$), LUMO + 1 ($1b_2$), and LUMO + 2 ($2a_1$). In the C_s symmetry of **8** and **9** they mix together giving the 1a′, 2a′, and 3a′ MOs. They are shown on the left side of Figures 5 and 6. The HOMO–LUMO interaction between **10** and **11** for the A and B geometries is shown in the upper part of Figures 5 and 6. For both conformations the resulting MO (1a′ + p_v^-) describes the Zr—C σ-bond. In the lower part of Figures 5 and 6 we show the interactions between the MOs 2a′ and 3a′ of **10** and the p_v^+ and σ_v MOs of **11**. It is clear that for the A-type geometry ($\alpha \ll 120°$) the resulting MOs (2a′ + p_v^+) and (3a′ + σ_v) describe the donor–acceptor β-CH agostic interaction (Figure 5). For the B-type geometry ($\alpha \gg 120°$) the same MOs describe the Si(C)—C_γ and C_γ—H agostic interactions (Figure 6). The calculated properties of the stabilizing interactions, present in both conformations A and B of **8** and **9**, are summarized in Tables V and VI. For the A-type geometry, the distortion leads to an increase of the electron density on the Zr atom, an increase of the overlap population of the bonds Zr—H_β and Zr—C_β, and a decrease of the electron density on C_β and H_β and of the overlap population in the CH_β σ-bond. All the above features confirm the existence of the β-CH agostic interactions in the A geometry of **8** and **9**. The β-CH agostic interactions stabilize **8** and **9** from 2.68 to 5.35 eV (Table V). The stabilization of the

---

(14) Albright, T. A.; Burdett, J. K.; Whangbo, M. H. In *Orbital Interactions in Chemistry*; Wiley: New York, 1985.

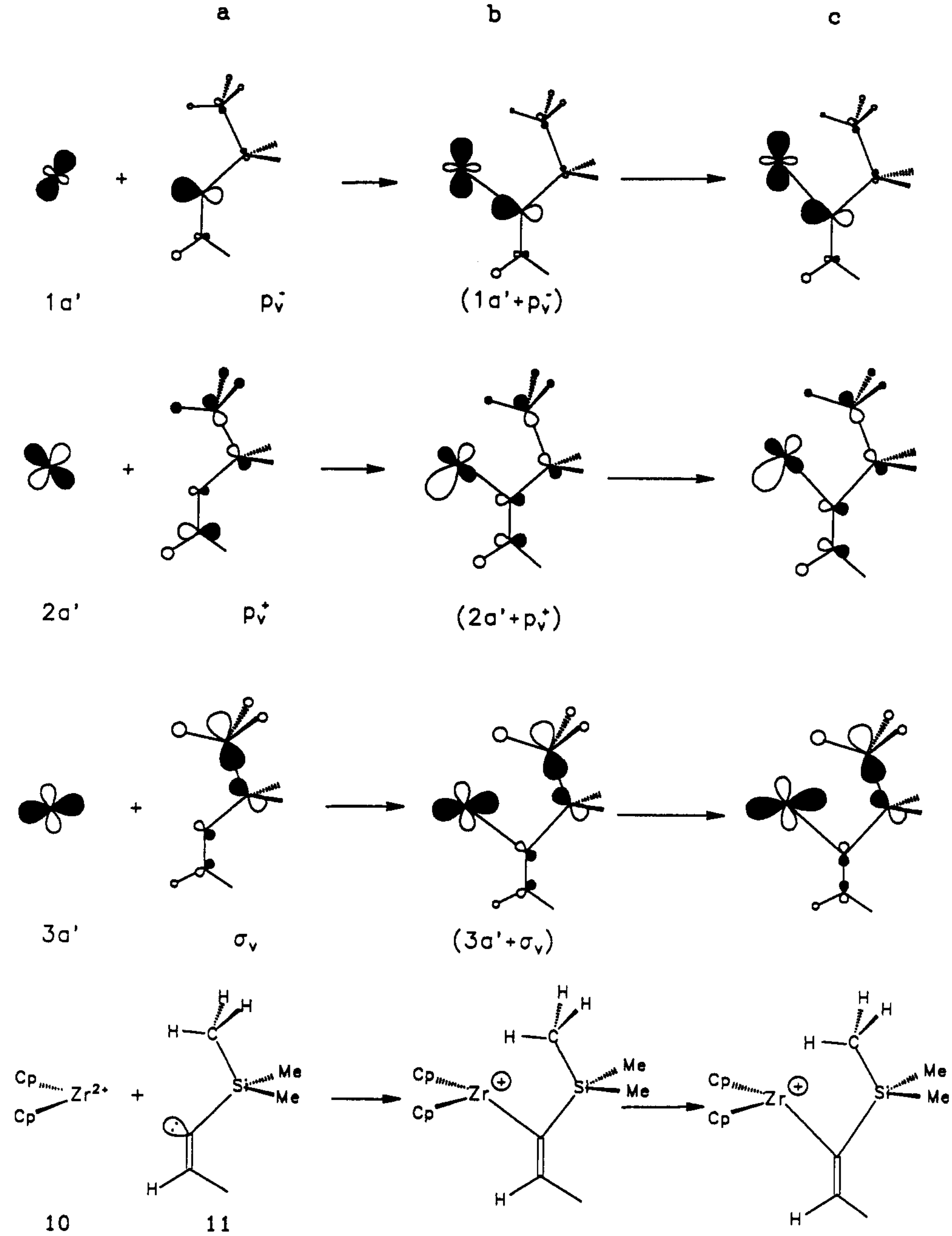

Figure 6. (a) Schematic drawing of the lowest unoccupied MOs of a Cp_2Zr^{2+} unit (**10**) and the highest occupied σ MOs of a $(CH_3)_3Si—C{=}CH_2^-$ unit (**11**). (b) Highest occupied σ MOs of **8a** (conformation B) assuming no agostic interaction. (c) Highest occupied σ MOs of **8a** assuming minimum B with agostic interactions.

complexes **9** is larger as compared to **8** with the same R_2. In Table V the substituents R_2 are ordered according to their group electronegativity.[15] It is noted that, with the exception of $R_2 = CMe_3$, ΔOP_{Zr-H} and ΔOP_{C-H} are roughly proportional to the group electronegativity of R_2.

Thus, both the steric and electronic factors of the substituents R_1 and R_2 have an influence of the β-CH agostic interactions. The complexes **9** with exception of **9a** and **9d** prefer β-CH agostic A-type structure. For **9d** ($R_2 = CMe_3$) the energy of both conformations A and B is of the same order, and **9a** (R_2 = H) prefers the B geometry. This allows us to suppose that the donor strength of the CC σ-bond is greater than of the CH σ-bond.

From the data presented in Table VI it follows that the stabilizing interactions involve two σ-bonds, i.e. C_γ–Si in **8** (or C_γ–C_β in **9**) and C_γ–H. The stabilization of the complexes **8** is greater as compared to **9** with the same R_2. We remember that all complexes **8** prefer the γ-C–Si agostic B-type structure (Table IV). It means that the $SiMe_3$ substituent differs considerably from the CMe_3 group. All above features allow us to suppose that the donor strength of the SiC σ-bond is greater than that of the CC σ-bonds. To find out how many C_γ–H σ-bonds are involved in the agostic interactions, we have carried out geometry optimizations on **1** and **12** for conformation B and B′, relaxing all bond angles of the ligand with the bond lengths fixed at experimental values.[6,16] The B′-type geometry differs from B by rotating the CH_3 group around the Si–C_γ bond. The results for **12** and the Ti complex are presented in Figure 7. It is noted that the

---

[15] Imamoto, N.; Masuda, S. *Chem. Lett.* **1982**, *1003*.

[16] We used the MOLEK-9000 Program Package by P. Bischof, Organisch-Chemisches Institut, University of Heidelberg.

Table V. Properties of Complexes 8 and 9 with the A-Type Structure[a]

		R_2					
A-type	R_1	SiH_3	$SiMe_3$	H	Me	CMe_3	Ph
ΔOP_{Zr-H}	$SiMe_3$	0.152	0.175	0.235	0.255	0.333	0.294
	CMe_3	0.142	0.189	0.210	0.252	0.289	0.276
ΔOP_{Zr-C}	$SiMe_3$	0.520	0.434	0.470	0.436	0.348	0.407
	CMe_3	0.526	0.392	0.511	0.421	0.349	0.415
ΔOP_{C-H}	$SiMe_3$	−0.108	−0.129	−0.216	−0.239	−0.351	−0.293
	CMe_3	−0.113	−0.170	−0.200	−0.247	−0.299	−0.282
Δq^{Zr}	$SiMe_3$	+0.27	+0.10	+0.18	+0.24	+0.28	+0.25
	CMe_3	+0.42	+0.39	+0.44	+0.34	+0.30	+0.45
Δq^{C}	$SiMe_3$	−0.38	−0.36	−0.38	−0.37	−0.41	−0.40
	CMe_3	−0.44	−0.44	−0.45	−0.42	−0.42	−0.45
Δq^{H}	$SiMe_3$	−0.08	−0.07	−0.08	−0.07	−0.05	−0.06
	CMe_3	−0.08	−0.07	−0.08	−0.07	−0.06	−0.06
ΔE_T (eV)	$SiMe_3$	4.95	4.50	2.68	4.48	5.27	3.55
	CMe_3	5.02	4.54	3.01	5.01	5.35	3.93

[a] OP = overlap population. $\Delta OP = OP(\alpha_{Min}) - OP(\alpha_{120°})$. $\Delta q = q(\alpha_{Min}) - q(\alpha_{120°})$ (positive sign means an increase of the electron density). $\Delta E_T = E_T(\alpha_{120°}) - E_T(\alpha_{Min})$.

Table VI. Properties of Complexes 8 and 9 with the B-Type Structure[a]

		R_2					
B-type	R_1	H	Me	SiH_3	CMe_3	$SiMe_3$	Ph
$\Delta OP_{Zr-C\gamma}$	$SiMe_3$	0.199	0.183	0.168	0.171	0.160	0.193
	CMe_3	0.153	0.126	0.133	0.124	0.135	0.138
$\Delta OP_{Zr-Si(C)}$	$SiMe_3$	0.098	0.080	0.073	0.071	0.069	0.090
	CMe_3	0.070	0.059	0.066	0.056	0.073	0.069
ΔOP_{Zr-H}	$SiMe_3$	0.229	0.177	0.171	0.152	0.176	0.219
	CMe_3	0.116	0.056	0.059	0.042	0.073	0.098
$\Delta OP_{C\gamma-Si(C)}$	$SiMe_3$	−0.058	−0.064	−0.057	−0.064	−0.050	−0.054
	CMe_3	−0.060	−0.061	−0.061	−0.062	−0.057	−0.057
$\Delta OP_{C\gamma-H}$	$SiMe_3$	−0.179	−0.142	−0.137	−0.123	−0.140	−0.172
	CMe_3	−0.111	−0.067	−0.070	−0.058	−0.081	−0.097
Δq^{Zr}	$SiMe_3$	+0.24	+0.15	+0.10	+0.11	+0.10	+0.23
	CMe_3	+0.26	+0.18	+0.21	+0.15	+0.26	+0.25
$\Delta q^{Si(C)}$	$SiMe_3$	−0.01	−0.01	0.00	0.00	+0.01	−0.01
	CMe_3	−0.12	−0.09	−0.10	−0.08	−0.11	−0.11
$\Delta q^{C\gamma}$	$SiMe_3$	−0.34	−0.30	−0.26	−0.27	−0.26	−0.33
	CMe_3	−0.16	−0.30	−0.11	−0.11	−0.12	−0.14
Δq^{H}	$SiMe_3$	−0.08	−0.07	−0.07	−0.06	−0.07	−0.08
	CMe_3	−0.09	−0.05	−0.05	−0.05	−0.06	−0.07
ΔE_T (eV)	$SiMe_3$	2.92	2.69	2.70	2.57	2.80	2.95
	CMe_3	2.37	2.01	2.11	1.94	2.23	2.28

[a] OP = overlap population. $\Delta OP = OP(\alpha_{Min}) - OP(\alpha_{120°})$. $\Delta q = q(\alpha_{Min}) - q(\alpha_{120°})$ (positive sign means an increase of the electron density). $\Delta E_T = E_T(\alpha_{120°}) - E_T(\alpha_{Min})$.

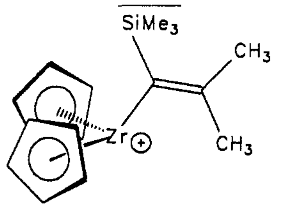

(4)

12

agreement with the experimental bond angles is good. Both complexes prefer a B-type conformation. This means that one CH σ-bond in the B geometry contributes more to the agostic interaction than two in the B′ conformation. The stabilizing contributions of two CH γ-bonds can only be achieved through interaction with the high lying a″ orbital of the metal fragment. The large energy gap makes this interaction negligible. Our results are in accord with experimental evidence found for **2**,[6b] but not with the theoretical investigation on model compounds for **1**.[7a] To the best of our knowledge no investigations on the C_γ–H agostic interactions in **1** have so far been reported.

Conclusions

Cp_2ML^+ are the intermediates in homogenous Ziegler–Natta catalysis. Various calculations[7a,11,17] as well as experimental work[18] have pointed to the possible role of three-center 2-electron M—X—C interaction for potentially stabilizing the active intermediate. Our study has revealed the factors important for the formation of such a stabilizing interaction and at the same time shown the limits of favorable M—H—C bond formation with regard to structure and substitution pattern at the metallocene/ligand system. In the cationic species, contrary to the neutral complexes, bulky substituents are not necessary to enforce the M—H—C bond formation. The stabilizing interactions present in $[Cp_2ZrC(R){=}CHR']^+$ are of

---

(17) (a) Castonguay, L. A.; Rappé, A. K. *J. Am. Chem. Soc.* **1992**, *114*, 5832. (b) Kawamura-Kuribayashi, H.; Koga, N.; Morokuma, K. *J. Am. Chem. Soc.* **1992**, *114*, 2359; **1992**, *114*, 8687. (c) Prosenc, M.-H.; Janiak, C.; Brintzinger, H.-H. *Organometallics* **1992**, *11*, 4036.

(18) (a) Kraudelat, H.; Brintzinger, H. H. *Angew. Chem.* **1990**, *102*, 1459; *Angew. Chem., Int. Ed. Engl.* **1990**, *29*, 1412. (b) Piers, W. E.; Bercaw, J. E. *J. Am. Chem. Soc.* **1990**, *112*, 9406.

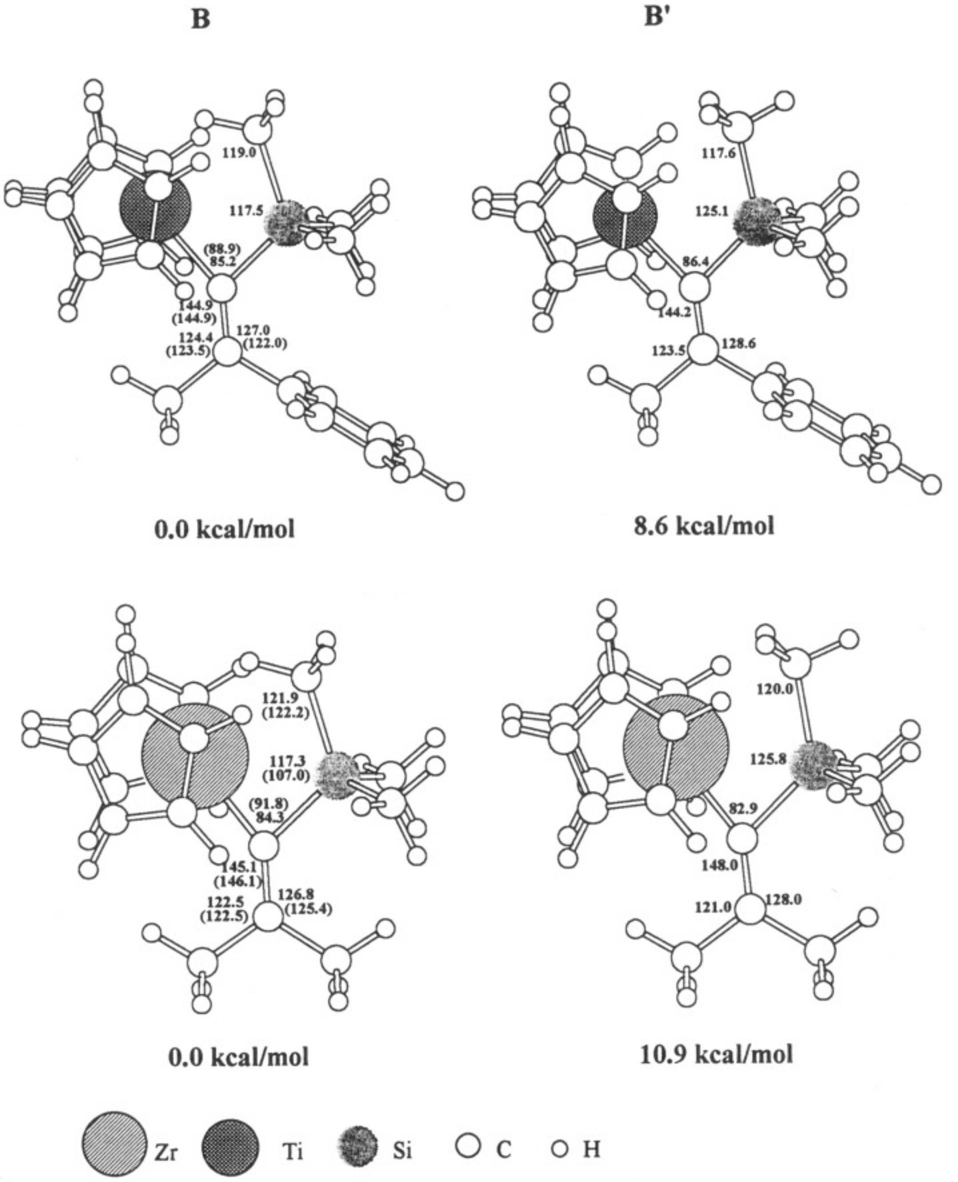

Figure 7. Optimized structures for **1** and **12** with two conformations of the CH_3 group (B and B′). The angles in parentheses correspond to the experimental values.

electronic origin, but its kind depends on a subtle balance between the electronic and steric features of R_1 and R_2.

If the Si–C σ-bond is accessible in R_1 the stabilization occurs via γ-C–Si agostic interaction, independently of R_2. If the C–C σ-bond is accessible in R_1 the stabilization occurs via β-CH agostic interaction, however, only in the presence of bulky R_2.

The subtle balance between the electronic and steric effects, depending on the substitution pattern of the alkene ligand can potentially influence the tacticity during olefin polymerization.

Acknowledgment. We are grateful to the Volkswagen-Stiftung, the Deutsche Forschungsgemeinschaft (SFB 247), and the Fonds der Chemischen Industrie for financial support.

OM9208230